Article published in *Nat. Chem.* (2017) 9, 676-680

DOI: https://doi.org/10.1038/nchem.2723

Link: https://www.nature.com/articles/nchem.2723

1000-Fold enhancement of high field liquid nuclear-magnetic resonance signals at room temperature

Guoquan Liu[1], Marcel Levien[2]†, Niels Karschin[2]†, Giacomo Parigi[3], Claudio Luchinat[3], Marina Bennati[1,2]*

[1]Electron-Spin Resonance Spectroscopy, Max Planck Institute for Biophysical Chemistry, Am Fassberg 11, 37077 Göttingen, Germany.

[2]Department of Chemistry, Georg-August-University, Tammannstr. 4, 37077 Göttingen, Germany.

[3]Magnetic Resonance Center (CERM) and Department of Chemistry, University of Florence, Via Luigi Sacconi 6, 50019, Sesto Fiorentino, Italy.

*Correspondence to: marina.bennati@mpibpc.mpg.de. † These authors contributed equally to this work.

Abstract: **Nuclear magnetic resonance (NMR) is a fundamental spectroscopic technique in structural studies of biological systems and materials, molecular imaging as well as analytical characterization of small molecules. It detects interactions at a very low energy scale and thus it is non-invasive and applicable to a variety of objects up to animals and**

humans. Despite of its achievements and unique potential, one of its most severe limitations is the low sensitivity, which stems from the small interaction energies involved. Among extensive efforts to overcome this limitation, progress in microwave technology has led dynamic nuclear polarization (DNP) to emerge as a promising tool to hyperpolarize nuclear spins for NMR. Nevertheless, in the liquid state this technique has been thought to be inherently limited by a decreasing efficiency towards high magnetic fields, at which modern NMR is performed. Here we report that DNP in liquid solution and room temperature can enhance the NMR signal of ^{13}C nuclei up to three orders of magnitude at magnetic fields around 3 Tesla. The experiment can be repeated fast (on the time scale of seconds) for signal averaging without introducing additional factors that interfere with the sample magnetic homogeneity. Thus, the method is compatible with conditions required by high resolution NMR for structural biology. Enhancement of ^{13}C signals on various organic compounds opens up new perspectives for DNP as a general tool to increase sensitivity in liquid NMR.

Addressing the sensitivity issue of NMR has been a long-standing goal in the field of magnetic resonance, which has continuously driven the community towards higher static magnetic fields, new detection technologies and more complex radio-frequency excitation schemes. Besides these conventional approaches, in the last decade the development of techniques that enhance the population difference between nuclear spin states (or their polarization) emerged as an active research area encompassing a variety of approaches[1-6]. Particularly, the transfer of polarization from electron spins to the magnetically coupled nuclear spin targets, called dynamic nuclear polarization (DNP), has become the most widespread tool to sensitize NMR spectroscopy [7,8]. In

liquids, DNP is driven by electron-nuclear cross relaxation resulting from fast molecular motion. For efficient cross relaxation the magnetic interaction between electron and nuclear spins has to be modulated at the electron spin resonance frequency. Liquid DNP experiments were first performed through detection of the ^{1}H nucleus [9], due to a larger sensitivity with respect to other nuclei. Since our first report at magnetic fields > 1 Tesla[10], some fundamental progress in ^{1}H DNP-NMR in liquids has been achieved[11-14]. However, small signal enhancements are always observed (< 10^2 at room temperature) at magnetic fields > 1 Tesla [11] because they originate from magnetic electron-nuclear dipole-dipole interaction predominantly modulated by molecular motions on the time scale of tens of ps [15].

To date, there has been little quantitative analysis of DNP-NMR enhancements of nuclei with lower gyromagnetic ratio, like ^{13}C and ^{15}N, because of the difficulty in their detection. However, it would be important to understand if ^{13}C nuclei can provide signal enhancements sizably larger than ^{1}H, as different sources of DNP could be present[16-20]. Taking advantage of an optimized DNP set up for 3.4 T/94 GHz [21] with a low power microwave source ($P_{MW} \leq 250$ mW), we addressed the question of whether ^{13}C signal enhancements are observable at high magnetic fields. By using nitroxide radicals as polarizer and achieving efficient saturation of the electron spin systems, we observed unprecedentedly large ^{13}C NMR signal enhancements.

Results and discussion

^{13}C-DNP enhancements. DNP experiments at a magnetic field of 3.4 Tesla were performed in various ^{13}C labelled compounds and solvents including CCl_4, $CHCl_3$ and $CDCl_3$, doped with ^{15}N labelled TEMPONE (4-oxo-2,2,6,6-tetramethylpiperidine-N-oxyl), for which DNP enhancements were reported at a lower field of 0.34 Tesla [17,22]. Use of ^{15}N TEMPONE is not essential but facilitates the saturation of the EPR line, due to the reduction of the three line EPR

spectrum (for ^{14}N TEMPONE) to a two-line spectrum with ^{15}N (see Fig. 1, inset). Details about the set up and the evaluation of DNP are given in SI1 and SI2. In all samples we observed at room temperature (RT) very large (> 10^2) positive DNP signal enhancements, which were sensitive to experimental conditions such as sample volumes, irradiation times and loaded resonator quality factor. The ^{13}C DNP-NMR spectrum of $^{13}CCl_4$ at 297 K after 15 s of MW irradiation (Fig. 1) shows an unprecedented signal enhancement of 930±100. We do not have evidence for temperature effects in these measurements, likely due to the small volume (≤ 500 nL) and the low dielectric constant of CCl_4. This was carefully controlled by comparison of the NMR signal build up rates $T_{\text{build up,}}$ with the nuclear spin-lattice relaxation time T_{1n}, which are expected to be comparable (SI3) [23].

FIGURE 1

The enhancement in Fig. 1 is significantly larger than that previously reported at a magnetic field of 5 Tesla for $^{13}CCl_4$ doped with BDPA ($\varepsilon \approx 40$)[20] and is even larger than that extrapolated by Dorn *et al*. [17] at 0.34 Tesla for the same polarizer/solvent system ($\varepsilon_{\mathbf{max}} = 770 \pm 115$). To our best knowledge, this is the highest directly (i.e. without extrapolations) reported enhancement in liquid-state DNP. The data also suggest that ^{13}C-DNP enhancements do not necessarily decrease with magnetic field, which is mechanistically new. To evaluate the DNP coupling factor ξ, we employ the Overhauser equation:

$$\varepsilon = 1 - \xi \cdot f \cdot s \cdot \frac{|\gamma_s|}{\gamma_I} \qquad (1)$$

where $\gamma_{S,I}$ are the gyromagnetic ratios of electron and nuclear spins, respectively, s is the saturation factor of the electronic spin system and f is a leakage factor [9]. We determined all

saturation and leakage factors independently, as described in SI3 and SI4. The resulting factors for CCl_4, $CHCl_3$ and $CDCl_3$ are listed in Table 1.

TABLE 1

The observed coupling factors $|\xi| = 0.4\text{-}0.5$ are 4-5 times larger than that for ^1H at the same field and temperature [21] and could in principle afford ^{13}C-DNP enhancements $> 10^3$ under conditions of $s, f \approx 1$, i.e. very high MW power and high polarizer concentrations (≥ 50 mM). Moreover, the coupling factors for $^{13}CHCl_3$ and $^{13}CDCl_3$ are similar, consistent with previous reports that polarization transfer mediated by the H atom (three-spin-effect) is negligible in samples with high polarizer concentration[18,22]. The negative value of the coupling factors is indicative of a DNP mechanism governed by the scalar (isotropic) hyperfine interaction, but $|\xi| < 1$ also points to partial contribution from dipolar interaction. Interestingly, Dorn *et al.* [17] reported much larger enhancements for $CHCl_3$ than for CCl_4 at 0.34 Tesla. This trend does not persist at ten times higher magnetic fields (3.4 Tesla).

^{13}C-DNP mechanism. To shed light into the ^{13}C-DNP mechanism we measured the enhancements (ε) of $^{13}CCl_4$ as a function of temperature. Fig.2A shows the dependence of ε on temperature in three samples with different concentrations. Only a small decrease with decreasing temperature is observed, corresponding to a less than 20% change at 243 K as compared to 297 K.

FIGURE 2

Analysis of the temperature behavior in Fig. 2A requires separation of the coupling factor $\xi(T)$ from the other temperature dependent terms, s and f (equation 1). At high magnetic fields the DNP coupling factor is expected to be given by (SI6):

$$\xi \approx \frac{-w_{0,s}}{w_{0,s}+2w_1} \qquad (2)$$

where $w_{0,s}$ is the relaxation probability for zero quantum transitions due to scalar interactions and $2w_1$ is the pure dipolar single-quantum transition probability [9]. Using equation 2 and introducing the expression for T_{1n} we can rewrite equation 1 as (SI6):

$$\frac{\varepsilon}{s \cdot T_{1n}} \approx w_{0,s} \cdot \left|\frac{\gamma_s}{\gamma_I}\right| \qquad (3)$$

According to equation 3, $w_{0,s}$ can be extracted from the enhancements when s and T_{1n} are determined independently (Supplementary Table 3). In Fig. 2B we have plotted $w_{0,s}(T)/w_{0,s}(297\ \mathrm{K})$ at each temperature calculated from $\varepsilon(T)/\varepsilon(297\ \mathrm{K})$ in Fig. 2A after correction for the respective s and T_{1n}. It becomes evident that $w_{0,s}$ decreases with increasing temperature in all four $^{13}CCl_4$ samples. To rationalize the temperature behavior of $w_{0,s}$ one has to recall its dependence on the spectral density $J(\omega_e)$ [9], which for a stochastic process is, or is close to, a Lorentzian function. The observed temperature behavior of $w_{0,s}$ falls into the regime of $\omega_e\tau_s \leq 1$, where $w_{0,s}$ increases with its correlation time τ_s. At 3.4 Tesla and an electron-spin resonance frequency ν_e = 94 GHz, $\omega_e\tau_s \leq 1$ is fulfilled for $\tau_s < 1.7$ ps. Such a short correlation time for scalar relaxation is consistent with the value proposed earlier by Müller-Warmuth and coworkers [16] from the analysis of ^{13}C DNP data at a field of 1 Tesla and was related to the average duration of a fast, elastic intermolecular collision, consistently with infrared and light scattering spectra [24].

More detailed understanding on the relaxation mechanisms can be obtained by nuclear-magnetic relaxation dispersion (NMRD), which measures the field dependence of the relaxivity ($1/T_{1n}$ normalized to 1 mM radical concentration) of target nuclei. In the $CHCl_3$ and CCl_4 samples (doped with nitroxide radical) at two temperatures (10 and 25° C), the ^{13}C relaxivity at 1

Tesla is more than 10 times lower than that at low fields (Fig. 3). This is in contrast to the relaxivity dominated by a diffusion-controlled dipolar interaction [15], where the value at high fields is theoretically 3/10 of that at low fields. This indicates that ^{13}C relaxation in $CHCl_3$ and CCl_4 is dominated by scalar hyperfine interaction with the nitroxide radicals, which is expected to decrease down to zero at high field. Furthermore, we note that the low field relaxivities of $CHCl_3$ and CCl_4 are quite different, which has to be related to the presence of a H atom in $CHCl_3$. A crude way to estimate the H-related contribution is to subtract 3/4 of the relaxivity of CCl_4 from that of $CHCl_3$ (Fig. 3). This H-related contribution has completely dispersed at ≥ 1 Tesla. Therefore, the high negative coupling factors observed at magnetic fields of 3.4 Tesla (Table 1) must be ascribed to scalar interactions mediated by the chlorine atoms, which are common to both $CHCl_3$ and CCl_4. We analyzed the relaxivity profiles using a so-called *pulsed* model [16], which assumes that the modulation of the scalar hyperfine interaction is controlled by the number of radical/solvent collisions through molecular diffusion (Poisson process) as well as by the length of the contact time (SI9). The NMRD profile of CCl_4 could be reproduced by one predominant (97%) type of collision with a contact time of $\tau_1 \sim 1$ ps and a small contribution (3%) of a second type of collision with $\tau_2 \sim 40$ ps (Fig.3, SI9). The contact time of ~ 1 ps is consistent with our experimental observation of $\tau_s < 1.7$ ps derived from Fig.2. The NMRD profile of $CHCl_3$ could be reproduced with the same parameters as CCl_4 plus the additional scalar contribution mediated by the H atom and a dipolar contribution arising from molecular diffusion (Supplementary Tables 6 & 7). The contribution from the H atom could be analyzed independently by fitting the difference curve in Fig.3. Using the *pulsed* model and fitting the parameters, the two coupling factors of $\xi = -0.47$ (CCl_4) and $\xi = -0.37$ ($CHCl_3$) at 3.4 Tesla could be well reproduced. The dipolar interactions result in only the term $2w_1$ in equation 2,

supporting our assumption. In summary, the present analysis provides a quantitative description of the DNP mechanism which includes a relevant contribution from a scalar interaction occurring through the chlorine atoms. A chlorine-mediated transfer of spin density was indeed predicted by quantum chemical calculations [25] leading to transient hyperfine interactions on the order of 10 MHz and even higher. These values could be reproduced by us using simple DFT calculations on a solvent-nitroxide complex (SI8).

^{13}C-DNP in biologically relevant compounds. To investigate the general applicability of ^{13}C DNP in high field liquid NMR, we examined molecules with ^{13}C chemical environments different from chlorinated carbons. Particularly, we selected ethyl acetoacetate and pyruvate as they are involved in several important metabolic pathways[26,27]. ^{13}C DNP enhancements on the order of 100 up to 300 were observed in the α-^{13}C carbons of ethyl acetoacetate, diethyl malonate and pyruvic acid (Fig. 4). We point out that the Boltzmann signal is far below the sensitivity limit (~2-5·10^{19} ^{13}C spins) of our EPR/DNP spectrometer (Table 2). Interestingly, a dipolar (negative) DNP enhancement is observed in the carbonyl carbons with no attached hydrogen (e.g. in diethyl malonate), and the enhancement is only 10-20% of the scalar DNP enhancement at the respective α-^{13}C. In all these experiments the saturation factor of the EPR line is still far from unity due to high dielectric losses. Therefore, the enhancements could be further improved if better saturation is achieved. Notably, we observed high scalar ^{13}C DNP enhancements in pyruvic acid for the first time. The significant scalar enhancements of the α-^{13}C carbons are rationalized by an efficient intermolecular hyperfine interactions mediated by the attached hydrogen. This is likely facilitated by the carbonyl group, which withdraws electron density from α-^{13}C and subsequently from the hydrogen α-^{13}C-H. This effect has been

previously more generally related by Dorn *et al*. [17] to the acid dissociation constant (pK_a) of the hydrogen atom attached to the target ^{13}C.

Conclusions. We have established that efficient ^{13}C-DNP at high magnetic fields (≥ 3 Tesla) is observable in a variety of liquid organic compounds. The key physical factor controlling the NMR signal enhancement is the subtle counteracting effect between dipolar and scalar relaxation in combination with the underlying molecular motion. We have shown that at high magnetic fields and suitable chemical environment, the contribution of dipolar relaxation is strongly attenuated allowing for large NMR signal enhancements. The capability to achieve enhancements up to three orders of magnitude with the ability to repeatedly enhance the signal by signal averaging should have a broad significance for various applications field of solution NMR, such as metabolomics studies, biological NMR for structure and dynamic of small molecules and potentially also for biological NMR of larger molecules, such as proteins. Particularly, the experiment can be repeated at room temperature without introducing additional factors interfering with the sample magnetic homogeneity. We expect that the future adaptation of the experimental set up to a high-resolution NMR magnet will also permit to preserve narrow NMR lines, as previously demonstrated in shuttle DNP experiments with detection at 14 Tesla.[11,22] Thus, the method is compatible with the conditions, under which high resolution NMR for structural biology is performed. Other emerging DNP-based hyperpolarization methods for liquids, such as dissolution DNP, deliver even larger enhancements (≥ 10^4) but are single-shot methods and to date limited to magnetic resonance imaging and medical applications[26,27]. Our results raise now the need of much broader investigations, such as the screening of signal enhancements in several compounds and proteins at even higher fields as well as thinking about suited devices for larger sample volumes. The present detection of a very efficient mechanism

for NMR signal enhancements in liquids at room temperatures and high magnetic fields opens up new perspectives for applications of liquid NMR spectroscopy, which would benefit greatly from higher sensitivity.

Methods

The DNP experiments were performed at a Bruker ElexSys E680 EPR spectrometer equipped with a Bruker AVANCE III 400 MHz NMR console. The superconducting 6 Tesla magnet is optimized for EPR experiments and does not provide shimming capabilities. A Bruker cylindrical resonator EN600-1021H with matched ENDOR coils for carbon NMR at ~36 MHz was employed. The samples were inserted into EPR capillaries with ID ranging from 0.2 mm to 0.7 mm, and were degassed by freeze-pump-thaw (1-2) cycles that efficiently removes O_2 and affords T_{1e} close or longer than 300 ns. For DNP, a liquid sample in a capillary was continuously irradiated by MW (Fig.1b) usually in resonance with the low-field hyperfine EPR transitions of ^{15}N-TEMPONE (Fig.1a) and the nuclear magnetization is subsequently measured with a one-pulse FID detection. For Boltzmann signal, the MW is switched off. To avoid heating of the resonator, a constant flow of N_2 gas is sometimes introduced to the cavity. More details are given in SI. NMRD measurements were obtained on a STELAR fast field-cycling relaxometer as previously described[15].

References

1. Ardenkjaer-Larsen, J. H. *et al.* Facing and overcoming sensitivity challenges in biomolecular NMR spectroscopy. *Angew. Chem. Int. Ed.* **54**, 9162-9185 (2015).
2. Rossini, A. J. *et al.* Dynamic nuclear polarization surface enhanced NMR spectroscopy. *Acc. Chem. Res.* **46**, 1942-1951 (2013).
3. Ni, Q. Z. *et al.* High frequency dynamic nuclear polarization. *Acc. Chem. Res.* **46**, 1933-1941 (2013).

4. Green, R. A. *et al.* The theory and practice of hyperpolarization in magnetic resonance using parahydrogen. *Prog. Nucl. Magn. Reson. Spectrosc.* **67**, 1-48 (2012).
5. Navon, G. *et al.* Enhancement of solution NMR and MRI with laser-polarized xenon. *Science* **271**, 1848-1851 (1996).
6. Bowers, C. R. & Weitekamp, D. P. Transformation of symmetrization order to nuclear-spin magnetization by chemical-reaction and nuclear-magnetic-resonance. *Phys. Rev. Lett.* **57**, 2645-2648 (1986).
7. Ardenkjaer-Larsen, J. H. *et al.* Increase in signal-to-noise ratio of > 10,000 times in liquid-state NMR. *Proc. Natl. Acad. Sci. U.S.A.* **100**, 10158-10163 (2003).
8. Hall, D. A. *et al.* Polarization-enhanced NMR spectroscopy of biomolecules in frozen solution. *Science* **276**, 930-932 (1997).
9. Hausser, D. & Stehlik, D. Dynamic nuclear polarization in liquids. *Adv. Magn. Reson.* **3**, 79-139 (1968).
10. Höfer, P. *et al.* Field dependent dynamic nuclear polarization with radicals in aqueous solution. *J. Am. Chem. Soc.* **130**, 3254-3255 (2008).
11. Griesinger, C. *et al.* Dynamic nuclear polarization at high magnetic fields in liquids. *Prog. Nucl. Magn. Reson. Spectrosc.* **64**, 4-28 (2012).
12. Franck, J. M., Pavlova, A., Scott, J. A. & Han, S. Quantitative cw Overhauser effect dynamic nuclear polarization for the analysis of local water dynamics. *Prog. Nucl. Magn. Reson. Spectrosc.* **74**, 33-56 (2013).
13. Prandolini, M. J., Denysenkov, V. P., Gafurov, M., Endeward, B. & Prisner, T. F. High-field dynamic nuclear polarization in aqueous solutions. *J. Am. Chem. Soc.* **131**, 6090-6092 (2009).
14. van Bentum, P. J. M., van der Heijden, G. H. A., Villanueva-Garibay, J. A. & Kentgens, A. P. M. Quantitative analysis of high field liquid state dynamic nuclear polarization. *Phys. Chem. Chem. Phys.* **13**, 17831-17840 (2011).
15. Bennati, M., Luchinat, C., Parigi, G. & Türke, M. T. Water 1H relaxation dispersion analysis on a nitroxide radical provides information on the maximal signal enhancement in Overhauser dynamic nuclear polarization experiments. *Phys. Chem. Chem. Phys.* **12**, 5902-5910 (2010).
16. Müller-Warmuth, W., Vilhjalmsson, R., Gerlof, P., Smidt, J. & Trommel, J. Intermolecular interactions of benzene and carbon tetrachloride with selected free radicals in solution as studied by 13C and 1H dynamic nuclear polarization. *Mol. Phys.* **31**, 1055-1067 (1976).

17. Wang, X. *et al.* Optimization and prediction of the electron-nuclear dipolar and scalar interaction in 1H and 13C liquid state dynamic nuclear polarization. *Chem. Sci.* **6**, 6482-6495 (2015).
18. Lingwood, M. D. & Han, S. G. Dynamic nuclear polarization of 13C in aqueous solutions under ambient conditions. *J. Magn. Reson.* **201**, 137-145 (2009).
19. George, C. & Chandrakumar, N. Chemical-shift-resolved 19F NMR spectroscopy between 13.5 and 135 MHz: Overhauser-DNP-enhanced diagonal suppressed correlation spectroscopy. *Angew. Chem. Int. Ed.* **53**, 8441-8444 (2014).
20. Loening, N. M., Rosay, M., Weis, V. & Griffin, R. G. Solution-state dynamic nuclear polarization at high magnetic field. *J. Am. Chem. Soc.* **124**, 8808-8809 (2002).
21. Türke, M. T., Tkach, I., Reese, M., Hofer, P. & Bennati, M. Optimization of dynamic nuclear polarization experiments in aqueous solution at 15 MHz/9.7 GHz: a comparative study with DNP at 140 MHz/94 GHz. *Phys. Chem. Chem. Phys.* **12**, 5893-5901 (2010).
22. Reese, M. *et al.* 1H and 13C dynamic nuclear polarization in aqueous solution with a two-Field (0.35 T/14 T) shuttle DNP spectrometer. *J. Am. Chem. Soc.* **131**, 15086-15087 (2009).
23. Türke, M. T. & Bennati, M. Comparison of Overhauser DNP at 0.34 and 3.4 T with Fremy's Salt. *Appl. Magn. Reson.* **43**, 129-138 (2012).
24. Bucaro, J. & Litovitz, T. Molecular motions in CCl4: light scattering and infrared absorption. *J. Chem. Phys.* **55**, 3585-3588 (1971).
25. Küçük, S. E. & Sezer, D. Multiscale computational modeling of 13C DNP in liquids. *Phys. Chem. Chem. Phys.* **18**, 9353-9357 (2016).
26. Jensen, P. R. *et al.* Hyperpolarized [1, 3 -13C2] ethyl acetoacetate is a novel diagnostic metabolic marker of liver cancer. *Int. J. Cancer* **136**, E117-E126 (2015).
27. Nelson, S. J. *et al.* Metabolic imaging of patients with prostate cancer using hyperpolarized [1-13C] pyruvate. *Sci. Transl. Med.* **5** (2013).

Acknowledgments

We would like to thank Roberto Rizzato for discussions on the initial ^{13}C-DNP experiments and Igor Tkach for technical support with the 94 GHz EPR spectrometer. Financial support has been provided by the Max Planck Society. G.L. thanks the Alexander von Humboldt Foundation for a fellowship. C.L. and G.P. acknowledge MIUR PRIN 2012SK7ASN, the European Commission, contracts BioMedBridges 284209 and pNMR 317127, and the EU ESFRI Instruct Core Centre CERM.

Author contributions

M.B., G.L. conceived and designed the research. G.L., N.K. and M.L. performed the 94 GHz DNP and EPR experiments. G.P. and C.L. performed and analyzed the NMRD experiments. G.L., G.P., C. L. and M.B. wrote the paper.

Additional information

Supplementary information is available in the on-line version of this paper. Reprints and permissions information is available at www.nature.com/reprints. Correspondence and requests for materials should be addressed to marina.bennati@mpibpc.mpg.de.

Competing financial interests

The authors declare no competing financial interests.

Table 1 Summary of DNP parameters in ^{13}C labelled solvents at 3.4 Tesla/94 GHz. Uncertainties in s, f and c are less than 5%, and 10 % for ε. Estimated errors in ξ are ≤ 15 %, however there is a small but significant, reproducible difference between CCl_4 and $CHCl_3$.

	c (mM)	$^{*}s$	f	$^{a}\varepsilon$	$^{b}\xi$
$^{13}CCl_4$	30	0.75	1	930±100	-0.47
$^{13}CHCl_3$	20	0.63	0.9	550±60	-0.37
$^{13}CDCl_3$	20	0.70	0.9	680±70	-0.41

*Values of s are likely upper limits as -for technical reason- the MW power in saturation transfer experiments (t_{irr} = 3-4 μs, SI4) is slightly larger than in the DNP experiments (t_{irr} = 1-15 s). Maximal values of s are consistent with our previous report on ^{1}H DNP ($s \approx 0.65$) in water solutions[21]. [a] Enhancements were achieved for MW irradiation times t_{irr} on the order of $3 \cdot T_{1n}$. [b]Because s and ε appeared underestimated, ξ might be at the lower limit of the 15 % error. Data for $CHCl_3$ and $CDCl_3$ are reported in SI2.

Table 2 Summary of DNP experiments in selected ^{13}C labelled compounds at 3.4 Tesla/94 GHz. MW irradiation length is 5 s. ^{15}N-TEMPONE concentration 20-40 mM. *Pyridine (1.5/1 M/M to pyruvic acid) is added to neutralize pyruvic acid to protect the nitroxide radical, but a radical decay during the DNP is still observed, which reduces the DNP enhancement. [a] and [b] correspond to the -$^{13}CH_3$ and -$^{13}CH_2$- peaks, respectively. Enhancement for ethyl acetoacetate-2,4-$^{13}C_2$ is estimated by comparison with a Boltzmann spectrum, as well as by comparison of the S/N to the detection sensitivity limit in our spectrometer (about 2-5·10^{19} spins). Both methods lead to a similar enhancement value. Enhancement for diethyl malonate-1,2,3-$^{13}C_3$ and pyruvic acid-3-^{13}C is estimated only by comparison of the S/N to the detection limit.

^{13}C labelled molecule	solvent	Mole ratio (M/M)	Vol. (nL)	No. of ^{13}C spins (10^{17})	No. of scans	S/N	Enhancement
ethyl acetoacetate-2,4-$^{13}C_2$	toluene	28:100	200	2 .0	32	8.5[a] 13.5[b]	150±50[a] 250±80[b]
diethyl malonate-1,2,3-$^{13}C_3$	toluene	35:100	200	2.5	128	21.5	200±60
pyruvic acid-3-^{13}C	di-isopropyl ether	77:100*	100	1.0	128	5.0	100±30

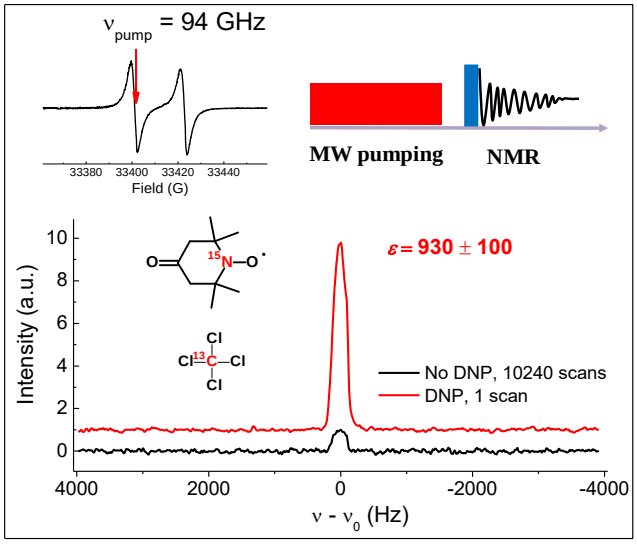

Figure 1 ^{13}C DNP-NMR experiments on $^{13}CCl_4$ doped with 30 mM ^{15}N-TEMPONE at 3.4 Tesla (ν_e = 94 GHz, ν_{NMR} (^{13}C) = 36 MHz, RT. Black: Boltzmann signal with 10240 scans and recycle delay of 15 s, and the spectrum scaled down by a factor of $10240^{1/2}$ for comparison at the same noise level to the DNP spectrum; Red: DNP with 1 scans and 15 s of MW irradiation ($P_{MW} \leq 250$ mW, $B_1 \leq 2$ G). Sample volume is ~500 nL. Inset left: 94 GHz EPR spectrum of TEMPONE at RT and the irradiation position of the pump pulse in the EPR line. Inset right: Schematic of a DNP experiment, in which a long resonant MW irradiation is followed by detection of the NMR signal.

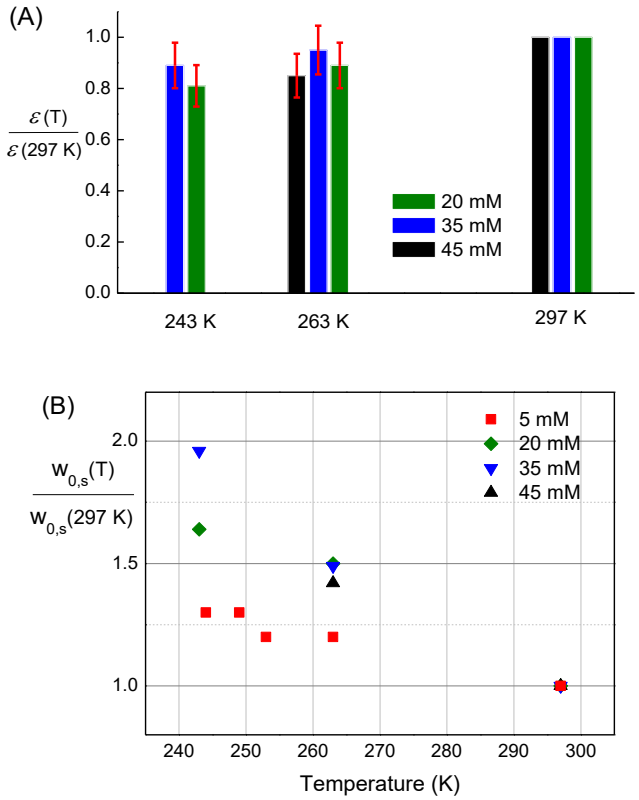

Figure 2 (**A**) Temperature dependence of the DNP enhancements (extrapolated from the DNP build up curve) in $^{13}CCl_4$. (**B**) Dependence of normalized scalar relaxivity on temperature in $^{13}CCl_4$. Relative errors are estimated to be 15%. The dielectric constant of CCl_4 is small (ε = 2.24) and possible temperature changes from MW irradiation are expected to be smaller than the temperature steps.

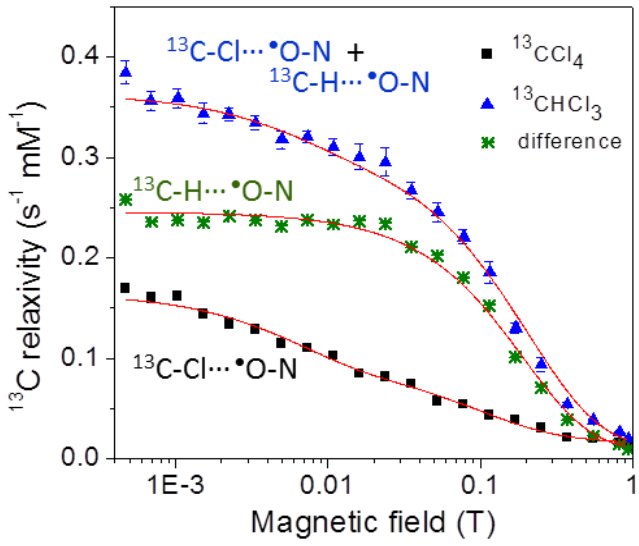

Figure 3 ^{13}C relaxivity of CCl_4 (black squares) and $CHCl_3$ (blue triangles) solutions of 200 mM TEMPONE. Green stars: Subtraction of 3/4 the relaxivity of CCl_4 from $CHCl_3$; The latter represents approximately the contribution due to the presence of the H atom in $CHCl_3$.

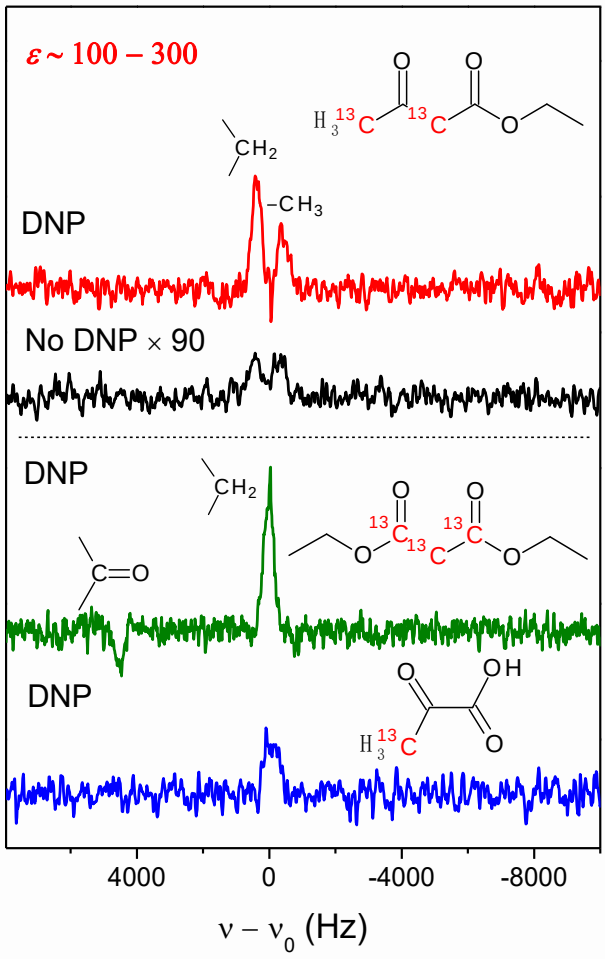

Figure 4 ^{13}C DNP-NMR (3.4 Tesla) spectra of ethyl acetoacetate (red), diethyl malonate (olive) and pyruvic acid (blue) doped with ~ 30-40 mM ^{15}N-TEMPONE. Black trace is the Boltzmann spectrum of an ethyl acetoacetate sample containing 3 times more ^{13}C of the corresponding DNP sample. The No. of accumulation scans for the Boltzmann spectrum is 900 time that of the DNP spectrum, and the spectrum is scaled down by a factor of $900^{1/2}$ for comparison at the same noise level to the DNP spectrum. In the DNP spectrum of diethyl malonate (olive), the negative NMR signal results from the carbonyl group dominated by dipolar DNP.